Analysis of the symmetry of a stressed medium using nonlinear elasticity

Rodrigo Felício Fuck & Ilya Tsvankin
Center for Wave Phenomena, Colorado School of Mines, Golden, CO 80401

ABSTRACT

Velocity variations caused by subsurface stress changes play an important role in monitoring compacting reservoirs and in several other applications of seismic methods. The most general way of describing stress-induced (or, equivalently, strain-induced) velocity fields is by employing the theory of nonlinear elasticity, which operates with third-order elastic (TOE) tensors. These sixth-rank strain-sensitivity tensors, however, are difficult to manipulate because of the large number of terms involved in the algebraic operations. Thus, even evaluation of the anisotropic symmetry of a medium under stress/strain proves to be a challenging task. Here, we employ a matrix representation of TOE tensors that allows computation of strain-related stiffness perturbations from a linear combination of 6×6 matrices scaled by the components of the strain tensor. In addition to streamlining the numerical algorithm, this approach helps to predict the strain-induced symmetry using relatively straightforward algebraic considerations. For example, our analysis shows that a transversely isotropic (TI) medium acquires orthorhombic symmetry if one of the principal directions of the strain tensor is aligned with the symmetry axis. Otherwise, the strained TI medium can become monoclinic or even triclinic.

Key words: anisotropic symmetry, nonlinear elasticity, stress-induced anisotropy, stiffness tensor, third-order elastic tensor, time-lapse seismic.

1 INTRODUCTION

Monitoring subsurface stress/strain fields and their time-lapse variations is an important research area with applications in velocity model-building (e.g., Sengupta and Bachrach, 2008) and reservoir geophysics (e.g., Fuck et al., 2009). For example, pore-pressure drop due to hydrocarbon production leads to reservoir compaction, which produces excess stress and strain not only in the reservoir itself, but also in the surrounding rock mass.

Seismic velocities can help to monitor subsurface stress and strain fields because numerous laboratory experiments have demonstrated that the stiffness tensor changes under stress/strain (Eberhart-Phillips et al., 1989; Prasad and Manghnani, 1997). In the elastic regime, stress stiffens grain contacts and closes fractures, making rocks more rigid and increasing P- and S-wave velocities. Therefore, some theoretical models describe the stress/strain sensitivity of seismic velocities through the stiffening of grain contacts (e.g., Gassman and Hertz-Mindlin models discussed in Mavko et al., 1998), while others relate the velocity variation to closing (or opening) of microcracks (e.g., Mavko et al., 1995; Sayers, 2006).

An alternative approach that has been successfully applied to this problem is based on the nonlinear theory of elasticity (e.g. Sinha and Kostek, 1996; Winkler et al., 1998; Sinha and Plona, 2001). In contrast to the Hertz-Mindlin theory, it employs a Taylor series expansion that yields the full elastic tensor of the strained medium (Thurston, 1974, p. 276). Unlike fracture-based models, nonlinear elasticity operates not with the fracture orientations and compliances, but with a third-order elastic (TOE) tensor responsible for the strain sensitivity of the rock mass.

We start by reviewing the nonlinear theory of elasticity and application of TOE tensors to model stress-

or strain-induced velocity changes. Then we use Voigt notation to represent TOE tensors as $6 \times 6 \times 6$ matrices and analyze the structure of these matrices for several common symmetry classes. This matrix representation naturally leads to an algebraic method to predict the anisotropic symmetry of the strained medium from the symmetry of the TOE tensor and the structure of the strain tensor. We use the proposed method to study the symmetry of a wide range of velocity models obtained by combining triclinic, monoclinic, orthorhombic, hexagonal and isotropic TOE tensors with several types of the strain tensor.

2 PHYSICAL MEANING OF TOE TENSORS

The nonlinear theory of elasticity (e.g. Thurston, 1974;Prioul et al., 2004), provides the most general way to model strain-induced velocity changes. The effective stiffness coefficients c_{ijkl} (each index runs from 1 to 3) of a medium under stress/strain can be expressed in terms of the stiffnesses (c°_{ijkl}) of the undeformed medium and the applied strains (Δe_{ij}) and stresses ($\Delta s_{ij} = c^{\circ}_{ijkl}\Delta e_{kl}$)*:

$$c_{ijkl} = c^{\circ}_{ijkl} + c_{ijklmn}\Delta e_{mn} + \Delta s_{ik}\delta_{jl} + c^{\circ}_{ijpk}\Delta e_{lp} + c^{\circ}_{ipkl}\Delta e_{jp}\,, \tag{1}$$

where the summation convention over repeated indices is implied, and δ_{jl} is Kronecker's symbol. The elements c_{ijklmn} form the so-called third-order elastic (TOE) tensor, which appears in the Taylor series expansion of the strain-energy function W:

$$W = W^{\circ} + s_{ij}e_{ij} + \frac{1}{2}c_{ijkl}e_{ij}e_{kl} + \frac{1}{6}c_{ijklmn}e_{ij}e_{kl}e_{mn} + O(e^4_{ij})\,. \tag{2}$$

Because of the structure of the third, fourth and fifth terms on the right-hand side of equation 1, the effective coefficients c_{ijkl} lose some of the symmetries of an elastic stiffness tensor (e.g., $c_{1313} \neq c_{3131}$). Nevertheless, ultrasonic experiments in rocks have shown that typically $\Delta s_{ij} \ll c_{ijkl} \ll c_{ijklmn}$ (Johnson and Rasolofosaon, 1996; Prioul et al., 2004), so the largest perturbation term in equation 1 is the one that contains the tensor c_{ijklmn}. Therefore, equation 1 can be simplified to

$$\begin{aligned} c_{ijkl} &= c^{\circ}_{ijkl} + c_{ijklmn}\,\Delta e_{mn} \\ &= c^{\circ}_{ijkl} + \Delta c_{ijkl}\,. \end{aligned} \tag{3}$$

The symmetry properties of the effective stiffness tensor c_{ijkl} in equation 3 ($c_{ijkl} = c_{jikl} = c_{ijlk} = c_{klij}$) coincide with those of the stiffness tensor for undeformed media. According to approximation 3, the symmetry of the tensor c_{ijkl} depends on the symmetries of the background medium (c°_{ijkl}) and the TOE tensor c_{ijklmn}, as well as on the structure of the strain tensor Δe_{mn}.

The large number of terms in equation 3 obscures the influence of the TOE and strain tensors on the stiffness perturbation Δc_{ijkl}. To facilitate analysis of strain-induced anisotropy, below we use a matrix representation of the main symmetry groups of the TOE tensor and recast equation 3 as a matrix-vector expression.

3 SYMMETRY OF THE TOE TENSOR

By analogy with the geometric symmetry of crystals, elastic tensors can be classified into different symmetry groups in accordance with the invariance of their components with respect to certain rotations of the coordinate frame (e.g., Helbig, 1994). Because of the symmetry of the strain and stress tensors, the coefficients c_{ijklmn} are invariant with respect to the permutation of the indices i and j, k and l, m and n. Hence, TOE tensors can be represented using Voigt notation, which maps every pair of indices ij into a single index α varying from 1 to 6:

$$\alpha = i\delta_{ij} + (9 - i - j)(1 - \delta_{ij})\,, \tag{4}$$

which yields

$$\begin{aligned} &11 \mapsto 1; \quad 22 \mapsto 2; \quad 33 \mapsto 3; \\ &12 \mapsto 6; \quad 13 \mapsto 5; \quad 23 \mapsto 4\,. \end{aligned} \tag{5}$$

In addition, because the strain-energy function W is invariant with respect to coordinate transformations, the coefficients c_{ijklmn} remain the same if the pairs ij, kl and mn are interchanged. In Voigt notation these symmetries can be succinctly written as

$$C_{\alpha\beta\gamma} = C_{\beta\gamma\alpha} = C_{\gamma\beta\alpha} = C_{\beta\alpha\gamma}\,. \tag{6}$$

Application of Voigt notation to second-order elastic (SOE) tensors c_{ijkl} helps to replace them by symmetric 6×6 matrices (e.g., Helbig, 1994). Likewise, TOE tensors expressed in Voigt notation are represented by $6 \times 6 \times 6$ matrices or a six-element vector composed of 6×6 matrices:

$$C_{\alpha(\beta\gamma)} = \begin{pmatrix} C_{1(\beta\gamma)}\,, C_{2(\beta\gamma)}\,, & C_{3(\beta\gamma)}\,, C_{4(\beta\gamma)}\,, C_{5(\beta\gamma)}\,, \\ & C_{6(\beta\gamma)} \end{pmatrix}^{\mathsf{T}}.$$

Fumi (1951, 1952) and Hearmon (1953) describe the linearly independent elements of the TOE tensor

*Equation 1 is derived from the wave-equation (Thurston, 1974), assuming that strains are measured from the underformed state, because we wish to measure the velocity changes caused by deformation. Strains could, of course, be measured in relation to other set of coordinates, for example, those describing the material points after the deformation. That would cause equation 1 to be slightly different (e.g., Sinha, 1982).

for all possible symmetry classes. Here, we use their results to construct the matrix representation for several symmetries relevant in the context of exploration geophysics. We proceed from the lowest possible symmetry (triclinic), which is characterized by the absence of any symmetry elements (i.e., symmetry axes or planes), to the isotropic tensor, which is invariant with respect to any coordinate transformation. A more detailed analysis of the matrices $C_{\alpha\beta\gamma}$ for various symmetry classes can be found in Appendix A.

3.1 Triclinic symmetry

Although the triclinic TOE tensor contains no symmetry elements, only 56 out of a total of $3^6 = 729$ elements are independent (equation 6). All six matrices that form the vector $C_{\alpha(\beta\gamma)}$ in equation **??** are symmetric because the indices β and γ can be interchanged:

$$C_{\alpha(\beta\gamma)} = \begin{pmatrix} C_{\alpha11} & C_{\alpha12} & C_{\alpha13} & C_{\alpha14} & C_{\alpha15} & C_{\alpha16} \\ C_{\alpha12} & C_{\alpha22} & C_{\alpha23} & C_{\alpha24} & C_{\alpha25} & C_{\alpha26} \\ C_{\alpha13} & C_{\alpha23} & C_{\alpha33} & C_{\alpha34} & C_{\alpha35} & C_{\alpha36} \\ C_{\alpha14} & C_{\alpha24} & C_{\alpha34} & C_{\alpha44} & C_{\alpha45} & C_{\alpha46} \\ C_{\alpha15} & C_{\alpha25} & C_{\alpha35} & C_{\alpha45} & C_{\alpha55} & C_{\alpha56} \\ C_{\alpha16} & C_{\alpha26} & C_{\alpha36} & C_{\alpha46} & C_{\alpha56} & C_{\alpha66} \end{pmatrix}; \tag{7}$$

$\alpha = 1, 2 \ldots, 6$.

3.2 Monoclinic symmetry

The matrix representation of monoclinic TOE tensors can be derived from equation 7 by defining either a plane of mirror symmetry or a 2-fold symmetry axis (Winterstein, 1990).† The independent elements $C_{\alpha\beta\gamma}$ are invariant with respect to rotation by $\theta = \pi$ around the symmetry axis; the same set of independent $C_{\alpha\beta\gamma}$ can be obtained by using a symmetry plane perpendicular to this axis. If the horizontal plane $[x_1, x_2]$ is the plane of symmetry, the monoclinic TOE matrices for $\alpha = 1$, 2, 3, and 6 have the following form (Appendix A):

$$C_{\alpha(\beta\gamma)} = \begin{pmatrix} C_{\alpha11} & C_{\alpha12} & C_{\alpha13} & 0 & 0 & C_{\alpha16} \\ C_{\alpha12} & C_{\alpha22} & C_{\alpha23} & 0 & 0 & C_{\alpha26} \\ C_{\alpha13} & C_{\alpha23} & C_{\alpha33} & 0 & 0 & C_{\alpha36} \\ 0 & 0 & 0 & C_{\alpha44} & C_{\alpha45} & 0 \\ 0 & 0 & 0 & C_{\alpha45} & C_{\alpha55} & 0 \\ C_{\alpha16} & C_{\alpha26} & C_{\alpha36} & 0 & 0 & C_{\alpha66} \end{pmatrix}. \tag{8}$$

†A direction is called a k-fold symmetry axis when a tensor is invariant with respect to rotations by $\theta = 2\pi/k$ around it (Helbig, 1994).

When $\alpha = 4$ or 5,

$$C_{\alpha(\beta\gamma)} = \begin{pmatrix} 0 & 0 & 0 & C_{\alpha14} & C_{\alpha15} & 0 \\ 0 & 0 & 0 & C_{\alpha24} & C_{\alpha25} & 0 \\ 0 & 0 & 0 & C_{\alpha34} & C_{\alpha35} & 0 \\ C_{\alpha14} & C_{\alpha24} & C_{\alpha34} & 0 & 0 & C_{\alpha46} \\ C_{\alpha15} & C_{\alpha25} & C_{\alpha35} & 0 & 0 & C_{\alpha56} \\ 0 & 0 & 0 & C_{\alpha46} & C_{\alpha56} & 0 \end{pmatrix}. \tag{9}$$

Interestingly, the matrices described by equation 8 have the same structure (i.e., the same nonzero elements) as the matrix representing the monoclinic SOE tensor (e.g., Helbig, 1994). The matrices in equation 9, however, contain nonzero elements in place of the vanishing elements in equation 8. According to equations 8 and 9, the total number of independent elements $C_{\alpha\beta\gamma}$ for monoclinic symmetry is 32.

3.3 Orthorhombic symmetry

Orthorhombic symmetry is characterized by three orthogonal 2-fold symmetry axes, or, correspondingly, by three orthogonal mirror symmetry planes (Helbig, 1994). Because orthorhombic symmetry is a special case of the monoclinic model, the matrix representation of the orthorhombic TOE tensor can be obtained from equations 8 and 9 by requiring invariance with respect to rotations by $\theta = \pi$ around the x_1- and x_2-axes. These constraints reduce the number of independent elements to 20, and, when $\alpha = 1$, 2, and 3, the orthorhombic matrices $C_{\alpha\beta\gamma}$ can be written as (see Appendix A)

$$C_{\alpha(\beta\gamma)} = \begin{pmatrix} C_{\alpha11} & C_{\alpha12} & C_{\alpha13} & 0 & 0 & 0 \\ C_{\alpha12} & C_{\alpha22} & C_{\alpha23} & 0 & 0 & 0 \\ C_{\alpha13} & C_{\alpha23} & C_{\alpha33} & 0 & 0 & 0 \\ 0 & 0 & 0 & C_{\alpha44} & 0 & 0 \\ 0 & 0 & 0 & 0 & C_{\alpha55} & 0 \\ 0 & 0 & 0 & 0 & 0 & C_{\alpha66} \end{pmatrix}. \tag{10}$$

For $\alpha = 4$, 5, and 6,

$$C_{4(\beta\gamma)} = \begin{pmatrix} 0 & 0 & 0 & C_{144} & 0 & 0 \\ 0 & 0 & 0 & C_{244} & 0 & 0 \\ 0 & 0 & 0 & C_{344} & 0 & 0 \\ C_{144} & C_{244} & C_{344} & 0 & 0 & 0 \\ 0 & 0 & 0 & 0 & 0 & C_{456} \\ 0 & 0 & 0 & 0 & C_{456} & 0 \end{pmatrix}, \tag{11}$$

$$C_{5(\beta\gamma)} = \begin{pmatrix} 0 & 0 & 0 & 0 & C_{155} & 0 \\ 0 & 0 & 0 & 0 & C_{255} & 0 \\ 0 & 0 & 0 & 0 & C_{355} & 0 \\ 0 & 0 & 0 & 0 & 0 & C_{456} \\ C_{155} & C_{255} & C_{355} & 0 & 0 & 0 \\ 0 & 0 & 0 & C_{456} & 0 & 0 \end{pmatrix}, \tag{12}$$

$$C_{6(\beta\gamma)} = \begin{pmatrix} 0 & 0 & 0 & 0 & 0 & C_{166} \\ 0 & 0 & 0 & 0 & 0 & C_{266} \\ 0 & 0 & 0 & 0 & 0 & C_{366} \\ 0 & 0 & 0 & 0 & C_{456} & 0 \\ 0 & 0 & 0 & C_{456} & 0 & 0 \\ C_{166} & C_{266} & C_{366} & 0 & 0 & 0 \end{pmatrix} . \tag{13}$$

As was the case for monoclinic symmetry, the matrices $C_{\alpha\beta\gamma}$ with $\alpha = 1, 2$ and 3 have the same structure (i.e., the same nonzero elements) as the orthorhombic SOE matrix.

3.4 Hexagonal symmetry

According to Hearmon (1953), there are two types of TOE tensors with hexagonal symmetry. The first type is defined by a 6-fold symmetry axis perpendicular to a mirror symmetry plane. The second (higher symmetry) type is obtained from the orthorhombic model by introducing a 6-fold symmetry axis perpendicular to one of the three orthogonal symmetry planes. Hereafter, we consider only TOE tensors of the second type.

The independent elements $C_{\alpha\beta\gamma}$ for type 2 hexagonal symmetry can be found by requiring that the matrix elements in equations 10–13 remain invariant with respect to a $2\pi/3$ rotation around the 6-fold symmetry axis, here assumed to point in the x_3-direction (more details are given in Appendix A). Note that if a certain element is invariant with respect to rotations of both $\theta = \pi$ (which is the case for the orthorhombic TOE tensor) and $\theta = 2\pi/3$ around the same axis, then it is also invariant with respect to rotations of $\theta = 2\pi/6 = \pi/3$.

Except for the matrix $C_{3(\beta\gamma)}$, all other matrices representing the TOE tensor with hexagonal symmetry have the same structure as those in equations 10–13. For hexagonal symmetry, however, the number of independent elements reduces to 10. The additional constraints are as follows[‡]:

$$C_{112} = C_{111} - C_{166} - 3C_{266} \, ; \tag{14}$$

$$C_{122} = C_{111} - 2C_{166} - 2C_{266} \, ; \tag{15}$$

$$C_{222} = C_{111} + C_{166} - C_{266} \, ; \tag{16}$$

$$C_{223} = C_{113} \, ; \tag{17}$$

$$C_{233} = C_{133} \, ; \tag{18}$$

$$C_{123} = C_{113} - 2C_{366} \, ; \tag{19}$$

$$C_{244} = C_{155} = C_{144} + 2C_{456} \, ; \tag{20}$$

$$C_{255} = C_{144} \, ; \tag{21}$$

$$C_{355} = C_{344} \, . \tag{22}$$

Equations 14–22 include nine independent elements of the TOE tensor; the tenth independent element is C_{333}.

[‡]These constraints are obtained from the scheme of Fumi (1952), as discussed in Appendix A.

Despite these constraints, $C_{1(\beta\gamma)}$ and $C_{2(\beta\gamma)}$ still retain the structure of the SOE matrix with orthorhombic symmetry. The matrix $C_{3(\beta\gamma)}$, on the other hand, has the VTI (transversely isotropic with a vertical symmetry axis) form:

$$C_{3(\beta\gamma)} = \begin{pmatrix} C_{113} & C_{123} & C_{133} & 0 & 0 & 0 \\ C_{123} & C_{113} & C_{133} & 0 & 0 & 0 \\ C_{133} & C_{133} & C_{333} & 0 & 0 & 0 \\ 0 & 0 & 0 & C_{344} & 0 & 0 \\ 0 & 0 & 0 & 0 & C_{344} & 0 \\ 0 & 0 & 0 & 0 & 0 & C_{366} \end{pmatrix} . \tag{23}$$

Thus, $C_{3(\beta\gamma)}$ does not have the same structure as $C_{1(\beta\gamma)}$ and $C_{2(\beta\gamma)}$, as was the case for the lower symmetries. It should be emphasized that in contrast to hexagonal SOE tensors, TOE tensors considered here are not "transversely isotropic" in the sense that they are not invariant with respect to arbitrary rotations around the 6-fold symmetry axis.

A similar pattern of matrix structures holds for $\alpha = 4$, 5, and 6. While $C_{6\beta\gamma}$ has the form described by equation 13, the constraints 20–22 show that $C_{4(\beta\gamma)}$ in equation 11 and $C_{5(\beta\gamma)}$ in equation 12 can be obtained from each other by permutation of columns and rows:

$$C_{5(\beta\gamma)} = \mathcal{R}_1 C_{4(\beta\gamma)} \mathcal{R}_1 \, , \tag{24}$$

where

$$\mathcal{R}_1 = \left(\begin{array}{c|c} P_1 & \mathbf{0} \\ \hline \mathbf{0} & P_1 \end{array} \right) . \tag{25}$$

Here, $\mathbf{0}$ is a 3×3 matrix of zeros and P_1 is a permutation matrix that interchanges the first and second columns or rows of any 3×3 matrix:

$$P_1 = \begin{pmatrix} 0 & 1 & 0 \\ 1 & 0 & 0 \\ 0 & 0 & 1 \end{pmatrix} . \tag{26}$$

3.5 Isotropic TOE

The isotropic TOE tensor is described by three linearly independent elements (e.g., Barsch and Chang, 1968), here chosen to be C_{123}, C_{144} and C_{456} (see Appendix A). The complete $C_{\alpha\beta\gamma}$ matrix for isotropic media can be expressed through just two matrices, $C_{1(\beta\gamma)}$ and $C_{4(\beta\gamma)}$:

$$C_{1(\beta\gamma)} = \begin{pmatrix} C_{111} & C_{112} & C_{112} & 0 & 0 & 0 \\ C_{112} & C_{112} & C_{123} & 0 & 0 & 0 \\ C_{112} & C_{123} & C_{112} & 0 & 0 & 0 \\ 0 & 0 & 0 & C_{144} & 0 & 0 \\ 0 & 0 & 0 & 0 & C_{155} & 0 \\ 0 & 0 & 0 & 0 & 0 & C_{155} \end{pmatrix} \tag{27}$$

and

$$C_{4(\beta\gamma)} = \begin{pmatrix} 0 & 0 & 0 & C_{144} & 0 & 0 \\ 0 & 0 & 0 & C_{155} & 0 & 0 \\ 0 & 0 & 0 & C_{155} & 0 & 0 \\ C_{144} & C_{155} & C_{155} & 0 & 0 & 0 \\ 0 & 0 & 0 & 0 & 0 & C_{456} \\ 0 & 0 & 0 & 0 & C_{456} & 0 \end{pmatrix}, \tag{28}$$

where (Thurston and Brugger, 1964)

$$C_{111} = C_{123} + 6C_{144} + 8C_{456}\,, \tag{29}$$
$$C_{112} = C_{123} + 2C_{144}\,, \tag{30}$$
$$C_{155} = C_{144} + 2C_{456}\,. \tag{31}$$

The remaining matrices can be obtained from the following permutations:

$$C_{2(\beta\gamma)} = \mathcal{R}_1 C_{1(\beta\gamma)} \mathcal{R}_1\,, \quad C_{3(\beta\gamma)} = \mathcal{R}_2 C_{1(\beta\gamma)} \mathcal{R}_2\,, \tag{32}$$
$$C_{5(\beta\gamma)} = \mathcal{R}_1 C_{4(\beta\gamma)} \mathcal{R}_1\,, \quad C_{6(\beta\gamma)} = \mathcal{R}_2 C_{4(\beta\gamma)} \mathcal{R}_2\,. \tag{33}$$

The matrix $\mathcal{R}_2$ has the same block structure as $\mathcal{R}_1$ from equation 25, but with P_1 substituted by P_2, a matrix that interchanges the first and third rows or columns of 3×3 matrices:

$$P_2 = \begin{pmatrix} 0 & 0 & 1 \\ 0 & 1 & 0 \\ 1 & 0 & 0 \end{pmatrix}. \tag{34}$$

4 SYMMETRY OF THE DEFORMED MEDIUM

The matrix representation of the TOE tensor helps to devise an algebraic procedure to evaluate the symmetry of a medium under stress/strain. Using Voigt notation, equation 3 can be expressed in terms of the TOE matrix $C_{\alpha\beta\gamma}$:

$$C_{\beta\gamma} = C^{\circ}_{\beta\gamma} + C_{\alpha\beta\gamma}\, \Delta E_\alpha\,, \tag{35}$$

where the vector $\Delta E_\alpha = (e_{11}, e_{22}, e_{33}, 2e_{23}, 2e_{13}, 2e_{12})^{\mathsf{T}}$ is obtained from the symmetric strain tensor Δe_{mn} by applying Voigt notation. Hereafter, the strain tensor with vanishing off-diagonal components ΔE_4, ΔE_5 and ΔE_6 will be called *diagonal*. If the elements ΔE_1, ΔE_2 and ΔE_3 of a diagonal strain tensor are equal, such a tensor represents *volumetric strain change* (Fuck et al., 2009).

Each perturbation stiffness element $\Delta C_{\beta\gamma} = C_{\alpha\beta\gamma}\, \Delta E_\alpha$ in equation 35 is obtained as a linear combination of the $C_{\alpha(\beta\gamma)}$ matrices scaled by the components of the vector ΔE_α. Due to the significant difference in the structure of the matrices $C_{\alpha(\beta\gamma)}$ for $\alpha = 1, 2, 3$ and $\alpha = 4, 5, 6$, it is possible to separate the contributions of the normal (diagonal) and shear (off-diagonal) strain components in equation 35. Next, we analyze the symmetry of the perturbation matrix $\Delta C_{\alpha\beta}$ using the results of the previous section. The structure of the resulting stiffness matrix $C_{\beta\gamma}$ is defined by the stiffnesses of the undeformed medium and the nonzero elements of $\Delta C_{\beta\gamma}$.

4.1 Isotropic TOE tensor

When the TOE tensor is isotropic, the symmetry of the matrix $\Delta C_{\alpha\beta}$ is entirely controlled by the structure of the strain tensor. This can be proved by substituting the matrix representation of the isotropic TOE tensor into equation 35.

For a volumetric strain change ($\Delta E_1 = \Delta E_2 = \Delta E_3$; $\Delta E_4 = \Delta E_5 = \Delta E_6 = 0$), the term $C_{\alpha\beta\gamma}\, \Delta E_\alpha$ reduces to the sum of the matrix $C_{1(\beta\gamma)}$ from equation 27 and its two permutations, $C_{2(\beta\gamma)}$ and $C_{3(\beta\gamma)}$, multiplied by the normal strain ΔE_1. The resulting tensor $\Delta C_{\alpha\beta}$ is isotropic:

$$\Delta C_{11} = \Delta C_{22} = \Delta C_{33} = (C_{111} + 2C_{112})\, \Delta E_1\,, \tag{36}$$
$$\Delta C_{44} = \Delta C_{55} = \Delta C_{66} = (C_{144} + 2C_{155})\, \Delta E_1\,, \tag{37}$$
$$\Delta C_{12} = \Delta C_{13} = \Delta C_{23} = \Delta C_{11} - 2\Delta C_{44} = (C_{123} + 2C_{111})\, \Delta E_1\,. \tag{38}$$

This confirms our expectation that any object undergoing volumetric change will remain just a scaled version of itself by conserving its original shape or symmetry.

If the applied strain is uniaxial, then the stiffness perturbation from equation 35 is transversely isotropic (TI). For example, the vertical strain ΔE_3 yields the tensor $\Delta C_{\alpha\beta}$ with VTI symmetry:

$$\Delta C_{11} = \Delta C_{22} = C_{112}\, \Delta E_3\,; \tag{39}$$
$$\Delta C_{33} = C_{111}\, \Delta E_3\,; \tag{40}$$
$$\Delta C_{44} = \Delta C_{55} = C_{155}\, \Delta E_3\,; \tag{41}$$
$$\Delta C_{66} = C_{144}\, \Delta E_3\,; \tag{42}$$
$$\Delta C_{12} = \Delta C_{11} - 2\Delta C_{66} = C_{123}\, \Delta E_3\,; \tag{43}$$
$$\Delta C_{13} = \Delta C_{23} = C_{112}\, \Delta E_3\,. \tag{44}$$

When the strain tensor is diagonal, each matrix $C_{\alpha(\beta\gamma)}$ ($\alpha = 1, 2, 3$) is multiplied with a different normal strain component, which results in the stiffness perturbation that has orthorhombic symmetry:

$$\Delta C_{\alpha\beta} = \begin{pmatrix} \Delta C_{11} & \Delta C_{12} & \Delta C_{13} & 0 & 0 & 0 \\ \Delta C_{12} & \Delta C_{22} & \Delta C_{23} & 0 & 0 & 0 \\ \Delta C_{13} & \Delta C_{23} & \Delta C_{33} & 0 & 0 & 0 \\ 0 & 0 & 0 & \Delta C_{44} & 0 & 0 \\ 0 & 0 & 0 & 0 & \Delta C_{55} & 0 \\ 0 & 0 & 0 & 0 & 0 & \Delta C_{66} \end{pmatrix}. \tag{45}$$

Furthermore, if the TOE tensor is isotropic, the symmetry of $\Delta C_{\alpha\beta}$ is always orthorhombic or higher, with the principal directions of the strain tensor defining the 2-fold symmetry axes of the deformed medium.

For example, a nonzero component ΔE_6 causes a rotation of the principal directions of the strain tensor around the x_3-axis of the Cartesian coordinate system. In addition to $C_{1(\beta\gamma)}$, $C_{2(\beta\gamma)}$ and $C_{3(\beta\gamma)}$, the stiffness perturbation for $\Delta E_6 \neq 0$ also depends on the matrix $C_{6(\beta\gamma)}$ (equation 35):

$$\Delta C_{\alpha\beta} = \begin{pmatrix} \Delta C_{11} & \Delta C_{12} & \Delta C_{13} & 0 & 0 & \Delta C_{16} \\ \Delta C_{12} & \Delta C_{22} & \Delta C_{23} & 0 & 0 & \Delta C_{26} \\ \Delta C_{11} & \Delta C_{12} & \Delta C_{13} & 0 & 0 & \Delta C_{36} \\ 0 & 0 & 0 & \Delta C_{44} & \Delta C_{45} & 0 \\ 0 & 0 & 0 & \Delta C_{45} & \Delta C_{55} & 0 \\ \Delta C_{16} & \Delta C_{26} & \Delta C_{36} & 0 & 0 & \Delta C_{66} \end{pmatrix}. \tag{46}$$

The matrix $\Delta C_{\alpha\beta}$ in equation 46 describes an orthorhombic medium rotated around the x_3-axis because ΔC_{16}, ΔC_{26}, ΔC_{36} and ΔC_{45} are linear combinations of stiffness perturbations in the unrotated coordinate system. For instance, the element ΔE_6 in the coordinate system rotated by the angle θ around the x_3-axis is given by

$$\Delta E_6 = 2\Delta e_{12} = 2(\Delta E_2' - \Delta E_1') \sin\theta\cos\theta\,, \tag{47}$$

where $\Delta E_1'$ and $\Delta E_2'$ denote the components of the strain tensor in the unrotated coordinate system. Using equation 47, we find that

$$\Delta C_{36} = \left(\Delta C_{23}' - \Delta C_{13}'\right) \sin\theta\cos\theta\,, \tag{48}$$

where $\Delta C_{ij}'$ are the components of the stiffness perturbation tensor in the unrotated coordinate system. Thus, the orientation of the vertical symmetry planes of the orthorhombic medium described by the matrix $\Delta C_{\alpha\beta}$ is determined by the element ΔE_6.

A numerical example of the stiffness perturbation $\Delta C_{\alpha\beta}$ that has orthorhombic symmetry resulting from the combination of a purely isotropic TOE tensor and an arbitrary (non-diagonal) strain tensor is given by Fuck et al. (2009). In their model, a pore-pressure drop inside a rectangular reservoir embedded in a homogeneous isotropic host rock induces stress/strain changes throughout the medium (Figure 1). The spatially varying stiffness perturbations caused by the excess stress/strain field are computed from equation 35. As illustrated by Figure 2, the compaction-related strain makes the reservoir and the surrounding medium both heterogeneous and anisotropic. In the vertical symmetry plane $[x_1, x_3]$ shown in Figures 1 and 2, the perturbation matrix $\Delta C_{\alpha\beta}$ corresponds to a transversely isotropic medium with elliptical P-wave anisotropy (i.e., the Thomsen parameters ε and δ are equal; Figure 2a). The accumulation of shear stress/strain near the corners of the reservoir causes a significant tilt of the symmetry axis from the vertical (Figure 2b).

4.2 Hexagonal TOE tensor

If the 6-fold symmetry axis is parallel to the x_3-direction, the matrix $C_{3(\beta\gamma)}$ of the hexagonal TOE tensor has VTI symmetry, whereas $C_{1(\beta\gamma)}$ and $C_2(\beta\gamma)$ are orthorhombic (equations 10 and 23). Therefore, a uniaxial strain applied in the symmetry-axis direction (i.e., $\Delta E_3 \neq 0$) yields the stiffness perturbation with VTI symmetry. If a uniaxial strain is parallel to the x_1- or x_2-axis, the stiffness perturbation inherits the orthorhombic symmetry of either the $C_{1(\beta\gamma)}$ or the $C_{2(\beta\gamma)}$ matrix. Furthermore, any diagonal strain tensor also produces $\Delta C_{\alpha\beta}$ with orthorhombic symmetry.

Volumetric strain ($\Delta E_1 = \Delta E_2 = \Delta E_3$) leads to VTI symmetry of the matrix $\Delta C_{\alpha\beta}$, because summation of the matrices $C_{1(\beta\gamma)}$, $C_{2(\beta\gamma)}$ and $C_{3(\beta\gamma)}$ results in the well-known VTI relationships:

$$\Delta C_{11} = \Delta C_{22} = (2C_{111} - C_{166} - 3C_{266} + C_{113})\,\Delta E_1\,, \tag{49}$$

$$\Delta C_{12} = \Delta C_{11} - 2\Delta C_{66} = (C_{112} + C_{122} + C_{123})\,\Delta E_1\,, \tag{50}$$

$$\Delta C_{13} = \Delta C_{23} = (C_{113} + C_{123} + C_{133})\,\Delta E_1\,, \tag{51}$$

$$\Delta C_{44} = \Delta C_{55} = (C_{144} + C_{155} + C_{344})\,\Delta E_1\,. \tag{52}$$

If the only non-vanishing shear strain is $\Delta E_6 = 2\Delta e_{12}$, the matrix $\Delta C_{\alpha\beta}$ still has orthorhombic symmetry, but its vertical symmetry planes are rotated with respect to the axes x_1 and x_2. This can be verified by showing that the elements ΔC_{45} and ΔC_{i6} ($i = 1, 2, 3$) are not linearly independent (e.g., equation 48 remains valid). The presence of nonzero shear strains defined in planes that are not perpendicular to the 6-fold symmetry axis of the TOE tensor lowers the symmetry of the stiffness perturbation. For instance, when $\Delta E_5 \neq 0$ ($\Delta E_4 = \Delta E_6 = 0$), ΔC_{46} no longer represents a linear combination of $\Delta C_{66}'$ and $\Delta C_{44}'$ because

$$\Delta C_{46} \neq \left(\Delta C_{66}' - \Delta C_{44}'\right) \sin\theta\cos\theta\,.$$

Then the symmetry of the perturbation $\Delta C_{\alpha\beta}$ becomes monoclinic with the $[x_1, x_3]$ symmetry plane. Similarly, if ΔE_4 is the only nonzero strain element, the perturbation stiffness tensor is also monoclinic, but the symmetry plane is $[x_2, x_3]$. If both ΔE_4 and ΔE_5 are nonzero, the perturbation $\Delta C_{\alpha\beta}$ has triclinic symmetry.

4.3 Lower TOE symmetries

The summation in equation 35 produces the stiffness perturbation that cannot have a higher symmetry than that of the TOE tensor. When the TOE tensor is orthorhombic or monoclinic, the symmetry of $\Delta C_{\alpha\beta}$ depends on the structure of the strain tensor only if the shear strains are nonzero. The combination of diagonal strain and the TOE tensor with orthorhombic or monoclinic symmetry always generates an orthorhombic or monoclinic stiffness perturbation $\Delta C_{\alpha\beta}$, respectively.

When the TOE tensor is orthorhombic, a single nonzero shear strain component produces the perturbation $\Delta C_{\alpha\beta}$ with monoclinic symmetry (equations 11–13). If two or three shear strains are nonzero, the result-

ing perturbation tensor is triclinic. Likewise, for a monoclinic TOE tensor, any shear strain not defined in the symmetry plane (i.e., in the plane perpendicular to the 2-fold symmetry axis) produces a triclinic perturbation $\Delta C_{\alpha\beta}$. Therefore, misalignment of the principal strain directions with the symmetry elements of the TOE tensor lowers the symmetry of $\Delta C_{\alpha\beta}$.

Finally, if the TOE tensor is triclinic (i.e., with no symmetry axes or planes), the stiffness perturbation always has triclinic symmetry as well, regardless of the structure of the strain tensor.

4.4 Symmetry of the resulting stiffness tensor

The above discussion was focused on the symmetry of the perturbation stiffness matrix $\Delta C_{\beta\gamma} = C_{\alpha\beta\gamma}\,\Delta E_\alpha$ in equation 35. Once this matrix has been obtained, it is straightforward to evaluate the symmetry of the effective elastic tensor $C_{\alpha\beta}$ which describes the medium after deformation. In principle, the symmetry of the strained medium should not be higher than that of either $C^\circ_{\alpha\beta}$ or $\Delta C_{\alpha\beta}$. There might be situations, however, in which some of the off-diagonal terms in $C^\circ_{\alpha\beta}$ and $\Delta C_{\alpha\beta}$ cancel out, resulting in the deformed medium with a higher symmetry than those of the background model and the stiffness perturbation. Although this issue should be studied further, such strain-induced compensation of intrinsic anisotropy seems unlikely.

5 CONCLUSIONS

Using the theory of nonlinear elasticity based on third-order elastic (TOE) tensors, we analyzed the symmetry of a medium under stress/strain. Application of Voigt notation leads to a convenient representation of the TOE tensor c_{ijklmn} in terms of a $6 \times 6 \times 6$ matrix $C_{\alpha\beta\gamma}$. The strain-induced stiffness perturbation $\Delta C_{\beta\gamma}$ is then obtained by summing 6×6 TOE submatrices scaled by the components of the strain tensor. This formalism provides a direct way to assess the contribution of each strain component to the stiffness perturbation for a given symmetry of the TOE tensor. In particular, our approach helps to separate the influence of the normal and shear strains on the symmetry of the perturbed medium.

In the simplest case of a purely isotropic TOE tensor, the perturbation $\Delta C_{\beta\gamma}$ always has orthorhombic or higher symmetry with the the 2-fold symmetry axes defined by the principal directions of the strain tensor. When the strain is uniaxial, the stiffness perturbation is transversely isotropic, and the symmetry axis is parallel to the strain direction. The deformed medium remains isotropic only if an isotropic TOE tensor is combined with volumetric strain (i.e., the strain tensor has only identical diagonal elements).

When the TOE tensor is hexagonal (transversely isotropic), a uniaxial strain applied in the direction of the symmetry axis conserves TI symmetry. If the strain tensor is diagonal or a uniaxial strain is confined to the plane orthogonal to the symmetry axis, the stiffness perturbation becomes orthorhombic. The influence of the off-diagonal (shear) strains may lower the symmetry of $\Delta C_{\beta\gamma}$ to monoclinic or even triclinic.

On the whole, our algebraic procedure significantly facilitates application of TOE tensors to analysis of strain-induced velocity perturbations. The formalism introduced here is as intuitive as that describing the strain sensitivity of seismic velocities through closing or opening of microcracks. Our results should be helpful in modeling and inversion of anisotropic velocity fields caused by excess strains/stresses near salt bodies and compacting hydrocarbon reservoirs.

6 ACKNOWLEDGMENTS

We are grateful to our colleagues in the Center for Wave Phenomena (CWP) at Colorado School of Mines (CSM) for helpful discussions. The constructive suggestions of the reviewers of *Geophysics* helped to improve the paper. This work was supported by the Consortium Project on Seismic Inverse Methods for Complex Structures at CWP.

References

Barsch, G. R., and Z. Chang, 1968, Second- and higher-order effective elastic constants of cubic crystals under hydrostatic pressure: Journal of Applied Physics, **39**, 3276–3284.

Eberhart-Phillips, D., D.-H. Han, and M. D. Zoback, 1989, Empirical relations among seismic velocity, effective pressure, porosity and clay content in sandstone: Geophysics, **54**, 82–89.

Fuck, R. F., A. Bakulin, and I. Tsvankin, 2009, Theory of traveltime shifts around compacting reservoirs: 3D solutions for heterogeneous anisotropic media: Geophysics, **74**, D25–D36.

Fumi, F. G., 1951, Third-orer elastic coefficients of crystals: Physical Review, **83**, 1274–1275.

——— 1952, Third-order elastic coefficients in trigonal and hexagonal crystals: Physical Review, **86**, 561.

Goldstein, H., 1980, Classical mechanics: Addison-Wesley, 2nd ed. edition.

Hearmon, R. F. S., 1953, Third-order elastic coefficients: Acta Crystallographica, **6**, 331–340.

Helbig, K., 1994, Foundations of anisotropy for exploration seismics: Pergamon.

Johnson, P. A., and P. N. J. Rasolofosaon, 1996, Nonlinear elasticity and stress-induced anisotropy in rock: Journal of Geophysical Research, **101**, 3113–3124.

Mavko, G., T. Mukerji, and J. Dvorkin, 1998, The rock physics handbook, tools for seismic analysis in

poroous media: Cambridge University Press, 1st edition.

Mavko, G., T. Mukerji, and N. Godfrey, 1995, Predicting stress-induced velocity anisotropy in rocks: Geophysics, **60**, 1081–1087.

Prasad, M., and M. H. Manghnani, 1997, Effects of pore and differential pressure on compressional wave velocity and quality factor in berea and michigan sandstones: Geophysics, **62**, 1163–1176.

Prioul, R., A. Bakulin, and V. Bakulin, 2004, Nonlinear rock physics model for estimation of 3d subsurface stress in anisotropic formations: theory and laboratory verification: Geophysics, **69**, 415–425.

Sayers, C. M., 2006, Sensitivity of time-lapse seismic to reservoir stress path: Geophysical Prospecting, **54**, 369–380.

Sengupta, M., and R. Bachrach, 2008, Velocity updating around salt bodies using stress modeling solutions and non-linear elasticity: 78th Annual International Meeting, SEG, Expanded Abstracts, 3048–3051.

Sinha, B. K., 1982, Elastic waves in crystals under a bias: Ferroelectrics, **41**, 61–73.

Sinha, B. K., and S. Kostek, 1996, Stress-induced azimuthal anisotropy in borehole flexural waves: Geophysics, **61**, 1899–1907.

Sinha, B. K., and T. J. Plona, 2001, Wave propagation in rocks with elastic-plastic deformations: Geophysics, **66**, 772–785.

Thurston, R. N., 1974, Waves in solids, *in* Truesdell, C., ed., Mechanics of Solids, *in* Flügge, S., Encyclopedia of Physics, **VI4a**, 109–308. Springer-Verlag.

Thurston, R. N., and K. Brugger, 1964, Third-order elastic constants and the velocity of small amplitude elastic waves in homogeneously stressed media: Physical Review, **133**, A1604–A1610.

Toupin, R. A., and B. Bernstein, 1961, Sound waves in deformed perfectly elastic materials. acoustoelastic effect: Journal of the Acoustical Society of America, **33**, 216–225.

Winkler, K. W., B. K. Sinha, and T. J. Plona, 1998, Effects of borehole stress concentrations on dipole anisotropy measurements: Geophysics, **63**, 11–17.

Winterstein, D. F., 1990, Velocity anisotropy terminology for geophysicists: geop, **55**, 1070–1088.

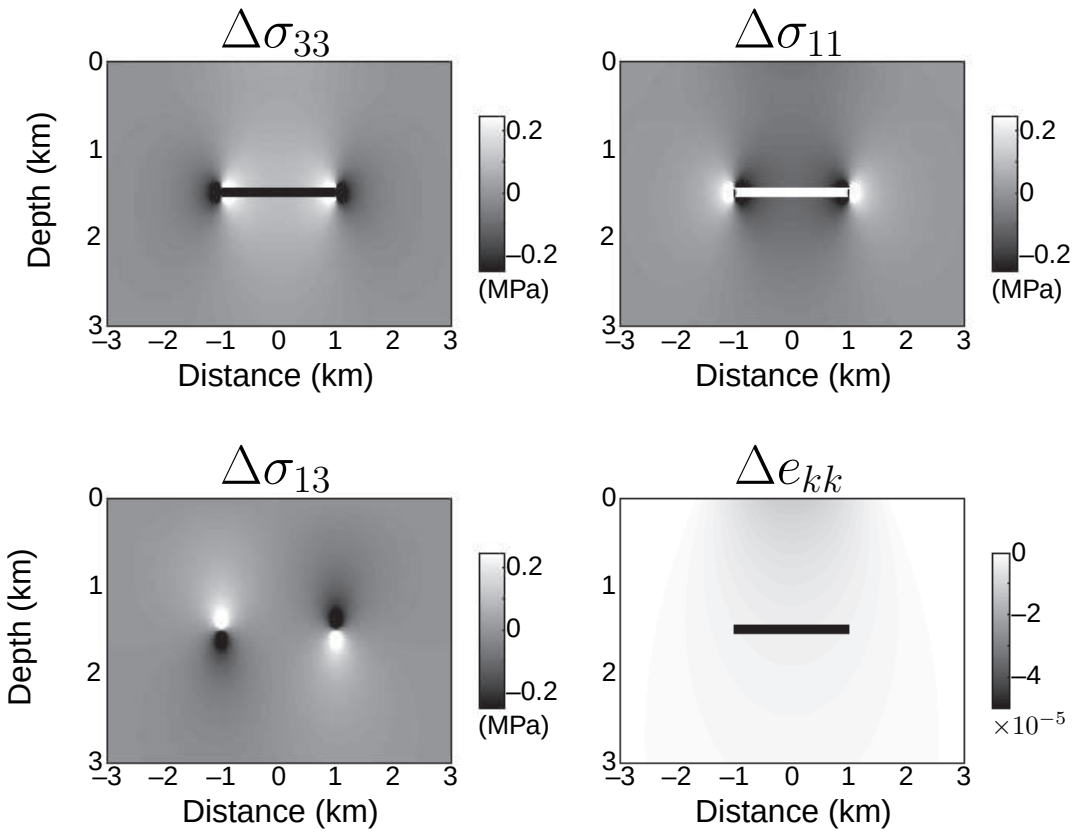

Figure 1. 2D stress and strain changes due to a 5 MPa drop in pore pressure inside a compacting rectangular reservoir (after Fuck et al., 2009). $\Delta\sigma_{33}$ and $\Delta\sigma_{11}$ are the normal deviatoric stresses, $\Delta\sigma_{13}$ is the shear deviatoric stress, and Δe_{kk} is the trace of the strain tensor. Negative values imply compression for stress and contraction (shortening) for strain. Inside the reservoir the maximum stresses are $\Delta\sigma_{33} = -2.2$ MPa and $\Delta\sigma_{11}$=1.7 MPa, while the volumetric change is constant: $\Delta e_{kk} = -4.6 \times 10^{-4}$. The plots were clipped for better visualization.

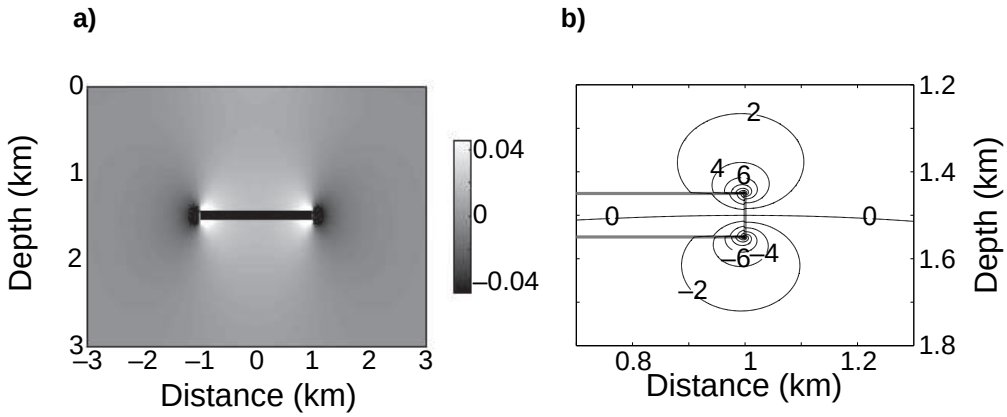

Figure 2. Anisotropy parameters and the symmetry-axis orientation of the strain-induced TI medium for the reservoir model from Figure 1 (after Fuck et al., 2009). a) The anisotropy parameter $\delta = \epsilon$ (color scale is clipped); b) contours of the angle between the symmetry axis and the vertical (positive angles correspond to clockwise axis rotation) near the right edge of the reservoir (gray rectangle). Inside the reservoir $\delta = -0.18$, while the tilt of the symmetry axis at the reservoir corners (where the shear strains become infinite) approaches $\pm 45°$ (for more details, see Fuck et al., 2009).

APPENDIX A: INDEPENDENT ELEMENTS OF THE TOE TENSOR

Here, we follow Fumi (1951, 1952) and Hearmon (1953) to describe the independent elements of the third-order elastic tensor for several common symmetry classes. Independent elements c_{ijklmn} for a given class should remain invariant with respect to rotations around a symmetry axis or reflections through a symmetry plane. According to the definition of a sixth-rank Cartesian tensor, such invariance implies that any independent element c_{ijklmn} should satisfy the following set of equations:

$$c_{ijklmn} - c_{pqrsuv} R_{ip} R_{jq} R_{kr} R_{ls} R_{mu} R_{nv} = 0\,, \quad \text{(A1)}$$

where R_{ij} is the unitary matrix describing the transformation of the tensor c_{ijklmn} due to a coordinate change. Equation A1 is used below to identify the set of independent elements for triclinic, monoclinic, orthorhombic, hexagonal and isotropic TOE tensors starting with the lower symmetries[§].

A1 Triclinic symmetry

The number N of independent elements $C_{\alpha\beta\gamma}$ for triclinic media can be found from the symmetry properties in equation 6 by taking into account that each index changes from 1 to 6 (Toupin and Bernstein, 1961):

$$N = \binom{6+3-1}{3} = \frac{8!}{3!\,5!} = 56\,. \quad \text{(A2)}$$

These 56 independent elements populate six full 6×6 symmetric matrices (equation 7).

A2 Monoclinic symmetry

For monoclinic media, only a subset of the 56 elements $C_{\alpha\beta\gamma}$ is independent. Since monoclinic symmetry has one mirror symmetry plane, the independent elements are the solutions of equation A1 written for a reflection with respect to this plane. Assuming that the symmetry plane is horizontal, the matrix R_{ij} in equation A1 is

$$\mathbf{R} = \begin{pmatrix} 1 & 0 & 0 \\ 0 & 1 & 0 \\ 0 & 0 & -1 \end{pmatrix}. \quad \text{(A3)}$$

Substituting equation A3 into equation A1, we find that each of the 56 equations reduces to:

$$c_{ijklmn} = (-1)^p c_{ijklmn}\,, \quad \text{(A4)}$$

where p is the number of times that the index 3 appears in c_{ijklmn}. Hence, only the elements c_{ijklmn} with an even number of indices 3 satisfy equation A4. The nonzero elements $C_{\alpha\beta\gamma}$ for monoclinic symmetry with a horizontal symmetry plane are listed in equations 8 and 9.

A3 Orthorhombic symmetry

Orthorhombic models are characterized by three orthogonal symmetry planes or, alternatively, by three orthogonal 2-fold symmetry axes. To identify the independent elements $C_{\alpha\beta\gamma}$, one can start with the monoclinic TOE tensor analyzed above and require invariance for reflection with respect to both vertical planes ($[x_1, x_3]$ or $[x_2, x_3]$). For example, the matrix R_{ij} for reflection with respect to the $[x_1, x_3]$-plane is

$$\mathbf{R} = \begin{pmatrix} 1 & 0 & 0 \\ 0 & -1 & 0 \\ 0 & 0 & 1 \end{pmatrix}. \quad \text{(A5)}$$

Substitution of equation A5 into equation A1 yields 32 equations (one for each independent element of the monoclinic tensor c_{ijklmn}). These equations have the form of expression A4, but the exponent p now stands for the number of times the index 2 appears in c_{ijklmn}. Therefore, the independent elements $C_{\alpha\beta\gamma}$ for orthorhombic symmetry should have an even number of indices 2 and 3. A similar procedure is applied to reflection with respect to the $[x_2, x_3]$-plane. The resulting matrix $C_{\alpha\beta\gamma}$, given in equations 10–13, has 20 independent elements.

A4 Hexagonal symmetry

To find out which components of the hexagonal tensor c_{ijklmn} are independent, we require that the elements c_{ijklmn} for orthorhombic media remain invariant with respect to rotation by $\theta = 2\pi/3$ around the axis x_3. The corresponding rotation matrix can be written as (Goldstein, 1980)

$$R = \begin{pmatrix} \cos\theta & \sin\theta & 0 \\ -\sin\theta & \cos\theta & 0 \\ 0 & 0 & 1 \end{pmatrix}. \quad \text{(A6)}$$

Because the matrix R has nonzero off-diagonal elements, equations A1 no longer reduce to a simple form similar to that of equation A4. Instead, one needs to solve systems of equations that relate certain groups of nonzero elements $C_{\alpha\beta\gamma}$. These systems can be obtained by transposing equations A1–A10 of Hearmon (1953).[¶]

From equations A1, A3 and A5–A7 of Hearmon (1953) one can deduce the constraints given in equations 14–22 above. Finally, we note that for any rotation around the x_3-axis, C_{333} always remains the same. Hence, it is the tenth (and last) independent element of the hexagonal TOE tensor.

[§]Helbig (1994) uses the same approach to identify the independent elements of SOE tensors.

[¶]This transposition is necessary because in our notation $C_{112} = c_{111122}$, as in Fumi (1952), and not $C_{112} = 3c_{111122}$, as in Hearmon (1953).

A5 Isotropy

A simple way of making the TOE tensor isotropic is to require that the 10 independent elements of the hexagonal tensor remain unchanged for arbitrary rotation around any axis. For example, c_{ijklmn} should stay the same when we interchange any two indices. Hence,

$$C_{111} = C_{222} = C_{333}; \tag{A7}$$

$$C_{112} = C_{133} = C_{223} = C_{113} = C_{122} = C_{233}; \tag{A8}$$

$$C_{144} = C_{255} = C_{366}; \tag{A9}$$

$$C_{155} = C_{266} = C_{344} = C_{166} = C_{244} = C_{355}; \tag{A10}$$

Taking into consideration the constraints in equations 14–22, the identities in equations A7–A10 also imply that

$$C_{112} = C_{123} + 2C_{144}\,, \tag{A11}$$

$$C_{111} = C_{123} + 6C_{144} + 8C_{456}\,. \tag{A12}$$

Therefore, the isotropic TOE tensor is completely defined by three independent constants (C_{123}, C_{144} and C_{456}), as shown in several publications (e.g. Barsch and Chang, 1968). The matrix representation of the isotropic TOE tensor is given in equations 27–33.